Journal Name

Dynamic Article Links►

Cite this: DOI: 10.1039/c0xx00000x

www.rsc.org/xxxxxx

ARTICLE TYPE

Phenothiazine and Carbazole Substituted Pyrene Based Electroluminescent Organic Semiconductors for OLED Devices

Jagadish K. Salunke,[a, b] F. L. Wong,[c] Krishna Feron,[d] Sergei Manzhos,[e] Ming Fai Lo,[c] Durgaprasad Shinde,[a] Abhijeet Patil,[a] C. S. Lee,[c] V. A. L. Roy,*[c] Prashant Sonar*[f] , Prakash P. Wadgaonkar*[a]

Received (in XXX, XXX) XthXXXXXXXXX 20XX, Accepted Xth XXXXXXXXX 20XX

DOI: 10.1039/b000000x

Due to the easy availability, low cost and opportunities for exploiting reactions of bromo substituents, 1, 3, 6, 8-tetrabromopyrene has attracted major attention in organic electronics community for designing and constructing novel classes of pyrene based organic semiconducting functional materials. In the present work, 1, 3, 6, 8-tetrabromo pyrene was transformed into corresponding tetrasubstituted carbazole and phenothiazine derivatives using the classical Suzuki coupling reaction. These newly synthesized materials with carbazole substituent (**PY-CA**) and phenothiazine substituent (**PY-PH**) were characterised thoroughly and were successfully used as an active light-emitting layer in organic light emitting diodes which resulted in blue and green emission with promising device performance. **PY-CA** exhibited maximum brightness around 2500 cd/m^2 and power efficiency of 1.5 lm/W while **PY-PH** exhibited 2116 cd/m^2 brightness and power efficiency 0.45 lm/W respectively.

Introduction

Since the discovery of organic light emitting diodes (OLEDs), numerous classes of light emitting organic semiconductors have been designed and developed and these efforts are still continuing in order to find materials that are easy to synthesize and exhibit improved solution processability and high efficiency.[1-3] The OLED technology has been used successfully for flat panel display and solid-state lighting applications.[4,5] Still there is a demand for the development of efficient pure red, blue, and green light emitting materials for OLEDs. Blue light emitting materials are also one of the important key elements for fabricating white OLED devices. Conjugated building blocks such as antracene,[6] pyrene,[7] phenothiazine [8] and carbazole [9] have been successfully used for designing and synthesizing light emitting active layers for OLED devices. However, current OLEDs still have some problems to get pure strong emission with lower power consumption which is determined by driving voltage and efficiency of the devices. Low driving voltage and high efficiency are required to reduce the power consumption of OLEDs.[10] In addition to the above issues, the electroluminescence properties of blue-emitting materials remain challenging,[11] particularly in terms of easy availability, lower cost, efficiency, stability, and color purity. Thus, it is very important to explore the new class of blue materials using various synthetic methodologies and potential starting precursor building blocks. Among such potential building blocks, pyrene conjugated system have attracted considerable interest in the designing of small organic molecules for different applications including OLEDs[12-15] and organic field effect transistors (OFETs)[16-19] due to its fused four aromatic condensed planar structure. Pyrene is a promising chromophore with higher fluorescent quantum yield which makes it an attractive candidate for designing functional materials for fluorescent probes and labeling experiments. Recently, N, N-di-p-methoxyphenylamine-substituted pyrene has been successfully used as a hole transporting materials for perovskite based solar cells with high efficiency. [20] These examples clearly reveal that pyrene is a versatile conjugated building block and can be used for designing a variety of conjugated functional materials. Pyrene posseses excellent thermal & chemical stability but on its own is not a good candidate for light emitting devices due to its excimer emission tendency which diminishes the fluorescence efficiency.[21,22] Nonetheless, this limitation of pyrene has been overcome by introducing bulky groups with long alkyl chains which enhances fluorescence quantum efficiency in OLEDs and also reduces the aggregation of the final material. [23] Over the last few years, our group has been exploring 1, 3, 6, 8 substituted pyrene based conjugated molecular functional materials for organic electronic devices. Initially, we reported a series of star-shaped organic semiconductors using bithiophene, phenylene, thienothiophene, and benzothiadiazole-thiophene chromophores. Among them, 1, 3, 6, 8-tetrakis (4-butoxyphenyl) pyrene, was used as the active emitting layer in simple solution-processed OLEDs with deep blue emission (CIE= 0.15, 0.18) and maximum efficiencies and brightness levels of 2.56 cd/A and 5000 cd/m^2, respectively.[24] In our second attempt, we synthesized single, double and triple bond incorporated three pyrene cored small conjugated molecules with octyloxy naphthalene conjugated substituent decorated at 1, 3, 6, 8 position of pyrene via Suzuki, Heck and Sonogashira coupling reactions, respectively. The effects of single, double and triple bonds on their optical, electrochemical, and thermal properties were studied in detail and all these materials were used successfully in OLEDs. [25] In the present work, we wish to report design, synthesis and characterization of two new compounds 1, 3, 6, 8-tetrakis(9-(4-

methoxyphenyl)-9H-carbazol-3-yl)pyrene (**PY-CA**) and 1, 3, 6, 8-tetrakis(10-(4-methoxyphenyl)-10H-phenothiazin-3-yl)pyrene (**PY-PH**). Although the carbazole and phenothiazine combination have been reported as an efficient deep blue and green emitting material in OLEDs earlier [26, 27] but so far there is no report in the literature about using them in the form of tetra-functionalized pyrene derivatives for any device application. Our results reveal that introduction of carbazole and phenothiazine unit on tetrabromopyrene core is the effective way to design wide band gap electroluminescent materials. Upon using these materials in OLED devices, carbazole substituted material exhibits blue emission with electroluminescent peak at 493 nm whereas phenothiazine substituted compound demonstrates green emission with electroluminescent peak at 540 nm. The highest brightness for carbazole and phenothiazine substituted pyrene was measured in OLED devices and which was found around 2500 cd/m^2 and 2116 cd/m^2 respectively. The reported OLED data clearly indicates that these classes of functional materials hold a great promise for designing future cost effective and efficient light emitting materials for OLED devices.

Experimental

All chemicals (palladium catalysts, bis (pinacolato) diboron, N-bromosuccinimide, 4-iodoanisole, potassium acetate and 1, 3, 6, 8-tetrabromopyrene) and solvents were purchased from Aldrich and were used without further purification. All the reactions were carried out using round bottom flask or Schlenk tube under an argon or nitrogen atmosphere in anhydrous solvents. ^{1}H and ^{13}C NMR spectra were recorded in $CDCl_3$ on Bruker AC spectrometer operating at 400 MHz for ^{1}H and 100 MHz for ^{13}C. The chemical shifts are referenced to tetramethylsilane (TMS). Matrix assisted laser desorption/ionization time-of flight (MALDI-TOF) mass spectra were obtained on a Bruker Autoflex TOF/TOF instrument using dithranol as a matrix. Melting points were recorded by open capillary method. UV-Vis and photoluminescence (PL) spectra were recorded on Jasco V-570, and Cary Eclipse Fluorescence spectrofluorometer, respectively using chloroform as a solvent.

Synthesis of 9H-carbazole-9-(4-methoxyphenyl) (2): Carbazole (2 g, 50 mmol), 4-iodoanisole (2.8 g, 60 mmol), copper powder (0.536 g, 50 mmol), potassium carbonate (2.7 g, 100 mmol) and triethylene glycol dimethyl ether (TEGDME) (30 mL) were added into Schlenk tube and the mixture was stirred under the argon atmosphere at 180 °C for 24 h. The reaction mixture was cooled to room temperature, filtered and poured into 500 mL of ice cold water. The white precipitate was collected by filtration. Recrystallization from 100 mL of methanol gave white crystalline solid (2,27 g, 70 % yield): (mp = 153-154 °C; lit. 154-155°C) [28].^{1}H NMR (400 MHz ,$CDCl_3$) δ = 8.14 - 8.01 (m, 2 H), 7.45 - 7.14 (m, 8 H), 7.08 - 6.98 (m, 2 H), 7.03 (d, J = 9.0 Hz, 9 H), 3.84 (s, 3 H). ^{13}C NMR (100 MHz, $CDCl_3$) δ = 141.3, 128.5, 125.8, 123.0, 119.9, 115.0, 109.6, 55.6.

Synthesis of 3-bromo-9-(4-methoxyphenyl)-9H-carbazole (3): 9H-Carbazole-9-(4-methoxyphenyl) (5 g, 10 mmol) was added into two necked round bottom flask containing chloroform (200 mL). After purging the reaction mixture for half an hour, N-bromosuccinimide (3,58 g, 12 mmol) was added and the reaction mixture was stirred for 12 hr at room temperature. The solution was poured into 500 mL of ice cold water and organic layer was extracted with 100 mL of dichloromethane. The combined organic layer was washed with 200 mL of water, dried over anhydrous sodium sulfate and filtered. Removal of solvent on a rotary evaporator afforded a crude product which was then chromatographed on silica with petroleum ether as an eluent to obtain title compound (5.51 g, 80 % yield), as a white solid. ^{1}H NMR (400 MHz, $CDCl_3$) δ = 8.29 (d, J = 1.5 Hz, 1 H), 8.12 (d, J = 7.8 Hz, 1 H), 7.60 - 7.41 (m, 4 H), 7.41 - 7.27 (m, 2 H), 7.26 - 7.09 (m, 3 H), 3.94 (s, 3 H).^{13}C NMR (100 MHz , $CDCl_3$) δ = 159.1, 140.9, 129.8, 127.1, 123.0, 122.1, 120.3, 115.2, 112.5, 111.2, 110.0, 77.1, 55.6.

Synthesis of 9-(4-methoxyphenyl)-3-(4,4,5,5-tetramethyl-1,3,2-dioxaborolan-2-yl)-9H-carbazole (4): 3-Bromo-9-(4-methoxyphenyl)-9H-carbazole (2 g, 1 mmol), bis(pinacolato)diboron (1.4 g, 1.2 mmol), $PdCl_2$(dppf) (418 mg, 0.1 mmol) and potassium acetate (1.6 g, 3 mmol) were added in Schlenk tube under argon flow and then evacuated for half an hour. Under an argon flow, anhydrous dioxane (25 mL) was added to the reaction mixture. The solution was stirred at room temperature for 30 min, and then at 80 °C for 24 h. The reaction mixture was quenched by addition of ice-cold water (250 mL) and then extracted with dichloromethane (250 mL). The dichloromethane solution was washed with water, dried over anhydrous sodium sulfate and filtered. Removal of solvent on a rotary evaporator afforded a crude product which was chromatographed on neutral alumina with 2% dichloromethane in petroleum ether as an eluent to obtain title compound (1.47 g, 65 % yield), as a yellow solid.^{1}H NMR (400 MHz , $CDCl_3$) δ = 8.63 (s, 3 H), 8.29 - 8.08 (m, 3 H), 7.84 (d, J = 8.2 Hz, 3 H), 7.53 - 7.20 (m, 19 H), 7.10 (d, J = 8.5 Hz, 6 H), 3.90 (d, J = 0.6 Hz, 3 H), 1.39 (s, 12 H). ^{13}C NMR (100 MHz, $CDCl_3$) δ = 159.5, 142.1, 132.9, 130.6, 128.7, 126.5, 123.7, 121.2, 115.7, 110.0, 84.2, 56.2, 25.5

Synthesis of 1,3,6,8-tetrakis(9-(4-methoxyphenyl)-9H-carbazol-3-yl)pyrene (PY-CA):1,3,6,8-Tetrabromopyrene (0.5 g, 1 mmol), 9-(4-methoxyphenyl)-3-(4,4,5,5-tetramethyl-1,3,2-dioxaborolan-2-yl)-9H-carbazole (2.31 g, 6 mmol), 2M K_2CO_3 (5 mL) and $Pd(PPh_3)_4$ (0.111 g, 0.1 mmol) were added in Schlenk tube under argon flow. The flask was evacuated and refilled with argon three times and then anhydrous THF (25 mL) was added into the flask and reaction mixture was stirred at 80 °C for 48 h. The reaction mixture was extracted with dichloromethane (250 mL) and washed with water (500 mL) and dried over anhydrous magnesium sulphate. Removal of solvent on rotary evaporator afforded a crude product which was then purified using silica gel column chromatography with 2% dichloromethane in petroleum ether as an eluent to obtain title compound **PY-CA** (0.969 g, 78% yield), as a green solid. 1H NMR (400 MHz ,) δ = 8.54 (s, 4 H), 8.38 (s, 10 H), 7.82 (d, J = 1.5 Hz, 4 H), 7.63 - 7.50 (m, 11 H),

7.49 - 7.38 (m, 9 H), 7.28 (s, 4 H), 7.21 - 7.13 (m, 8 H), 3.96 (s, 12 H).13C NMR (100 MHz , $CDCl_3$) δ = 158.9, 141.3, 137.8, 133.0, 129.6, 126.6, 123.0, 120.1, 115.1, 109.7, 55.6. MALDI-TOF: calculated 1288.00, found 1287.73.

Synthesis of 10-(4-methoxyphenyl)-10H-phenothiazine (6): A mixture of phenothiazine (2 g, 50 mmol), 4-iodoanisole (3.36 g, 60 mmol), copper powder (0.754 g, 50 mmol), potassium carbonate (3.30 g, 100 mmol), and triethylene glycol dimethyl ether (TEGDME) (30 mL) were added into Schlenk tube and the mixture was stirred under the argon atmosphere at 180 °C for 24 h. The reaction mixture was cooled to room temperature, filtered and poured into 250 mL of ice cold water. The brown precipitate was collected by filtration. The product was purified by recrystallization from ethyl acetate to afford yellowish crystalline solid (1.83 g, 60 % yield): (mp = 170 °C; lit. 172−173 °C) [29].^{1}H NMR (400 MHz , $CDCl_3$) δ = 7.54 - 7.36 (m, 2 H), 7.31 - 7.18 (m, 2 H), 7.18 - 7.07 (m, 2 H), 6.96 (dd, J = 2.1, 7.3 Hz, 4 H), 6.32 (d, J = 7.5 Hz, 2 H), 4.03 (s, 3 H).^{13}C NMR (100 MHz, $CDCl_3$) δ = 55.6, 115.7, 116.3,118.9, 122.6, 126.7, 127.4, 132.1, 132.6, 144.2, 159.1

Synthesis of 3-bromo-10-(4-methoxyphenyl)-10H-phenothiazine (7): 4-Phenothiazine-10-yl-anisole (2 g, 10 mmol) was added into 250 mL two necked round bottom flask containing chloroform (100 mL). After purging the reaction mixture with argon for half an hour, N-bromosuccinimide (1.28, 12 mmol) was added and the reaction mixture stirred for 12 h at room temperature. The reaction mixture was poured into 250 mL of ice cold water and extracted with dichloromethane. The dichloromethane solution was washed with water, separated and dried over sodium sulfate. Removal of solvent on rotary evaporator afforded a crude product which was then chromatographed on neutral alumina with 2% ethyl acetate in petroleum ether as an eluent to obtain title compound (2.14 g, 85% yield), as a green solid. ^{1}H NMR (400 MHz, $CDCl_3$) δ = 7.43 - 7.22 (m, 2 H), 7.22 - 7.07 (m, 3 H), 7.07 - 6.75 (m, 4 H), 6.21 (d, J = 8.3 Hz, 1 H), 6.05 (dd, J = 5.6, 8.8 Hz, 1 H), 3.92 (s, 3 H) ^{13}C NMR (100 MHz, $CDCl_3$) δ= 159.4, 158.9, 132.0, 129.6, 128.7, 126.9, 122.6, 116.9, 116.0, 55.6.

Synthesis of 10-(4-methoxyphenyl)-3-(4, 4, 5, 5-tetramethyl-1, 3, 2-dioxaborolan-2-yl)-10H-phenothiazine (8):

3-Bromo-10-(4-methoxyphenyl)-10H-phenothiazine (2 g, 1 mmol), bis(pinacolato)diboron (1.59 g, 1.2 mmol), $PdCl_2$(dppf) (383 mg, 0.1 mmol) and potassium acetate (1.5 g, 3 mmol) were added into Schlenk tube under argon flow and then evacuated for half an hour. Under an argon flow anhydrous dioxane (25 mL) was added to the reaction mixture. The solution was first stirred for 30 min at room temperature, and then at 80 °C for 24 h. The reaction mixture was quenched by addition of ice-cold water (250 mL) and then extracted with dichloromethane (250 mL). The dichloromethane solution was washed with water, dried over anhydrous sodium sulfate and filtered. Removal of solvent on rotary evaporator afforded a crude product which was chromatographed on neutral alumina with 2% dichloromethane in petroleum ether as an eluent to obtain title compound (1.21 g, 68% yield), as a green solid.^{1}H NMR (400 MHz , $CDCl_3$) δ = 7.42 (d, J = 1.4 Hz, 1 H), 7.35 – 7.19 (m, 3 H), 7.19 - 7.05 (m, 2 H), 6.97 (d, J = 9.1 Hz, 1 H), 6.80 (d, J = 3.8 Hz, 2 H), 6.14 (d, J = 8.0 Hz, 2 H), 3.91 (s, 3 H), 1.37 - 1.20 (m, 12 H) ^{13}C NMR (100 MHz , $CDCl_3$) δ = 159.2, 133.7, 132.9, 131.9, 126.6, 123.0, 122.5, 122.0, 115.3, 83.5, 55.5, 24.7.

Synthesis of 1,3,6,8-tetrakis(10-(4-methoxyphenyl)-10H-phenothiazin-3-yl)pyrene (PY-PH): 1,3,6,8-Tetrabromopyrene (0.5 g, 1 mmol), 10-(4-methoxyphenyl)-3-(4,4,5,5-tetramethyl-1,3,2-dioxaborolan-2-yl)-10H-phenothiazine (2.49 g, 6 mmol), 2M aqueous K_2CO_3 (5 mL) and $Pd(PPh_3)_4$ (0.111 g, 0.1 mmol) were added in Shlenck flask under argon flow. The flask was evacuated and refilled with argon three times and then anhydrous THF (25 mL) was added into the flask and reaction mixture was stirred at 80 °C for 48 h. The reaction mixture was extracted with dichloromethane (250 mL) and washed with water (500 mL) and dried over anhydrous sodium sulphate. Removal of solvent on rotary evaporator afforded a crude product which was then purified using silica gel column chromatography with 4% dichloromethane in petroleum ether as an eluent to obtain title compound **PY-PH** (0.819 g, 60% yield), as a yellow solid. ^{1}H NMR (400 MHz, $CDCl_3$) δ = 8.13 (s, 4 H), 7.85 (s, 2 H), 7.53 - 7.23 (m, 14 H), 7.22 - 6.95 (m, 16 H), 6.95 - 6.71 (m, 7 H), 6.44 - 6.13 (m, 8 H), 3.94 (s, 12 H)^{13}C NMR (100 MHz , $CDCl_3$) δ = 159.3, 143.9, 44.5, 135.9, 135.0, 133.3, 132.3, 128.5, 126.8, 125.1, 122.4, 119.6, 115.7, 55.6- MALDI-TOF: calculated 1415,04. found 1415.37

OLED Device Fabrication:

OLED devices were fabricated using **PY-CA** and **PY-PH** active emitting layer for evaluating the electroluminescent (EL) performance. The OLED device configuration glass/ITO/PEDOT: PSS/**PY-CA** or **PY-PH**/TPBi/Ca/Ag was used. Patterned ITO glass substrates were routinely cleaned by detergent and deionized water, then blown dry by nitrogen gas and kept in a 110 ^{o}C oven for 3 h before a 25 min ultra-violet ozone (UVO_3) surface treatment. Filtered poly (3, 4-ethylenedioxythiophene) polystyrene sulfonate (PEDOT: PSS) solution was spin-coated on the patterned ITO glass substrates and they were baked at 140 ^{o}C for 20 min. The thickness of the PEDOT: PSS films were controlled to 150 nm. Then **PY-CA** and **PY-PH** solutions prepared in chloroform were separately spin-coated on the individual PEDOT: PSS coated ITO glass substrates. They were baked at 70 ^{o}C for 20 min. The thickness of both **PY-CA** and **PY-PH** films were controlled to 20 nm. All the spin-coat processes were performed in nitrogen glove box environment. Both the **PY-CA** and **PY-PH** coated substrates were then loaded into a thermal evaporation chamber at vacuum pressure of below $3x10^{-6}$ Torr. 20 nm of 2, 2', 2"-(1, 3, 5-benzinetriyl)-tris (1-phenyl-1-H-benzimidazole) (TPBI), 20 nm of calcium (Ca) and 100 nm of silver (Ag) were coated on the substrates. With the completion of the device, EL measurements were carried out. The EL emission spectra were measured using PR650 CCD camera with a computer controller power supply The voltage-current-brightness (I-V-B) characteristics and the C.I.E. coordinates were also measured. The current and power efficiencies were calculated from the I-V-B data of the devices.

Cite this: DOI: 10.1039/c0xx00000x

www.rsc.org/xxxxxx

ARTICLE TYPE

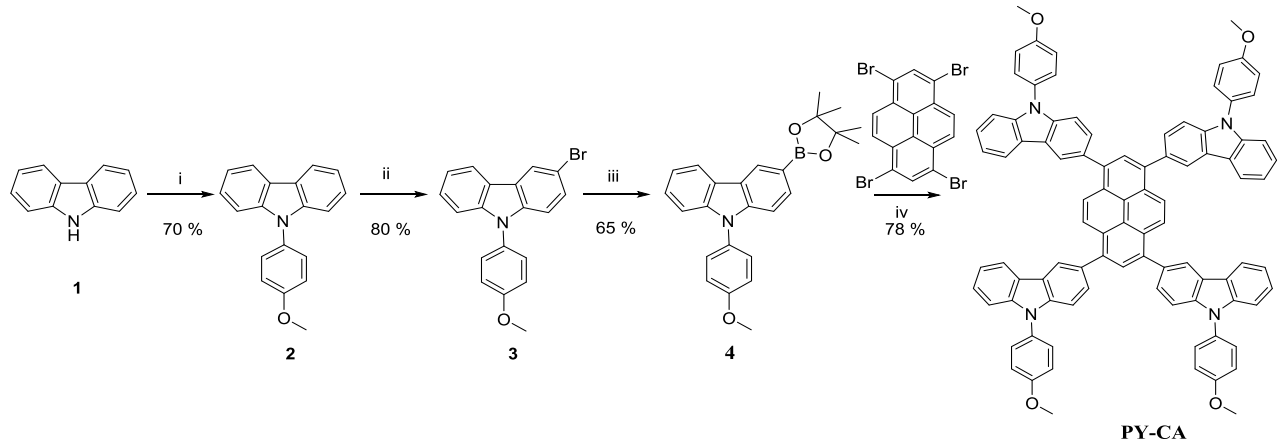

Scheme-1

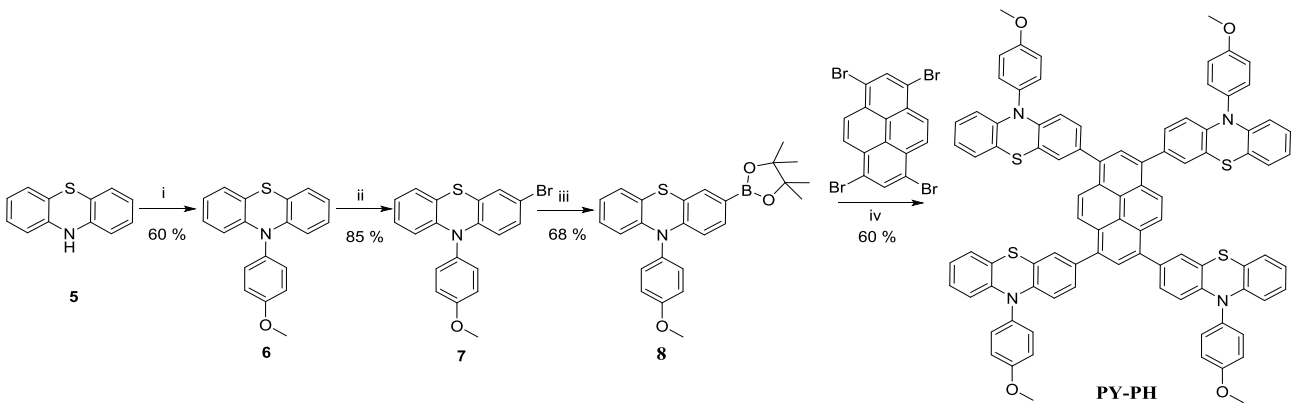

Scheme-2

Reagents:- (i) 4-Iodoanisole, DMSO, Cu, K_2CO_3,180°C, 24 h (ii) NBS, $CHCl_3$, R.T. 12h. (iii) Bis (pinacolato) diboron, Pd (dppf) Cl_2. KOAc, 80°C, 24 h. (IV) Pd $(PPh_3)_4$, K_2CO_3 (2M), THF, 80°C, 48 h.

Results and Discussion

In this work, two different conjugated segments *viz* carbazole and phenothiazine were selected for attachment to the central pyrene chromophore. In order to induce the solution processibility, a methoxyphenyl group was attached to both the carbazole and phenothiazine. First, commercially available compounds *viz*, carbazole (**1**) and phenothiazine (**5**) were converted to 9H-carbazole-9-(4-methoxyphenyl) (**2**) and 10-(4-methoxyphenyl)-10H-phenothiazine (**6**), respectively in 70% and 60% yield *via* Buchwald coupling using 4-iodoanisole. Compound 2 and 6 were then converted to their monobromo derivatives *viz* 3-bromo-9-(4-methoxyphenyl)-9H-carbazole (3) and 3-bromo-10-(4-methoxyphenyl)-10H-phenothiazine (**7**) using standard bromination conditions. Subsequent transformation of mono bromo compounds (**3**) and (**7**) to their respective bisboronic ester analogs 9-(4-methoxyphenyl)-3-(4,4,5,5-tetramethyl-1,3,2-dioxaborolan-2-yl)-9H-carbazole (**4**) and 10-(4-methoxyphenyl)-3-(4,4,5,5-tetramethyl-1,3,2-dioxaborolan-2-yl)-10H-phenothiazine (**8**) was carried out using bis(pinacolato)diboron reagent. The target compounds 1, 3, 6, 8-tetrakis(9-(4-methoxyphenyl)-9H-carbazol-3-yl)pyrene (**PY-CA**) and 1,3,6,8-tetrakis(10-(4-methoxyphenyl)-10H-phenothiazin-3-yl)pyrene (**PY-PH**) were prepared in 78% and 60% yield *via* classical Suzuki coupling conditions using 1, 3, 6, 8-tetrabromopyrene and monoboronic ester analogs (**4**) and (**8**) respectively. Syntheses of both final pyrene compounds are shown in Scheme 1 and Scheme 2. Both the derivatives were readily soluble in common organic solvents such as dichloromethane, chloroform, toluene, tetrahydrafuan, etc. This allowed purification of these compounds by column chromatography. The purity of all the synthesized precursors as well as final semiconductors were confirmed by ^1H NMR, ^{13}C NMR and MALDI-TOF spectroscopy (see all the data in Supporting Information). The optical properties of **PY-CA** and **PY-PH** compounds were characterized in solution (chloroform)

by both UV-vis absorption (UV) and photoluminescence (PL) spectroscopy (Figure 1). UV-vis spectra of both compounds exhibit two absorption peaks respectively at shorter and longer wavelengths. The absorption in the 300 nm to 500 nm region clearly indicates the wide band gap nature of the compounds. **PY-CA** exhibits two absorbance peaks at 339 nm and 400 nm whereas **PY-PH** showed peaks at 340 nm and 450 nm, respectively. The near-identical peaks at 339 nm and 340 nm are the signature peaks for the central pyrene core and this is comparable with absorbance of molecular pyrene (338 nm). Compared to the pyrene core, **PY-CA** and **PY-PH** exhibits the higher wavelength peaks at 400 nm and 450 nm respectively, which were arise from the enhanced conjugation between pyrene core and the attached carbazole/phenothiazine moiety. The 50 nm red shift in **PY-PH** compared to **PY-CA** is due to the more extended conjugation length of phenothiazine than carbazole. Both compounds show red shift of about 60 and 100 nm, respectively, in their absorption maxima compared to the base pyrene compound in solution state. The solution of **PY-CA** and **PY-PH** under UV-lamp shows deep sky blue and green emission (see Supporting Information). The peaks of the PL spectra of **PY-CA** and **PY-PH** compounds were recorded at 450 nm and 500 nm, respectively. The observed PL maxima are 50 nm and 100 nm red shifted compared to the pyrene photoluminescence spectra (PL max 393 nm).

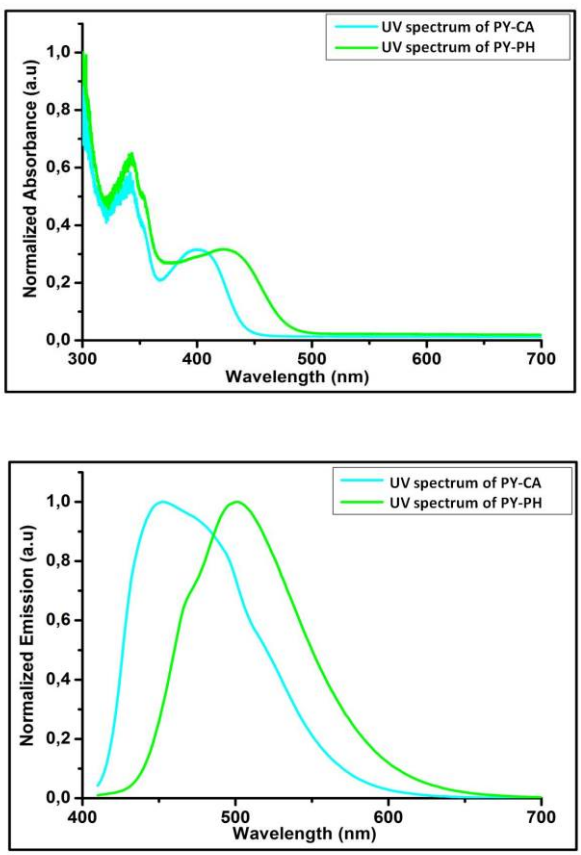

Figure 1. UV-vis absorption (upper) and photoluminiscence (lower) spectra of **PY-CA** and **PY-PH** compounds in chloroform solution (1x 10^{-4} M). PL was measured at the 370 nm excitation wavalenegth.

The thin film of **PY-PH** and **PY-CA** were spin coated on the separate quartz substrates and were measured by UV-vis and PL spectroscopy, which is shown in Figure 2**.** In the solid state, **PY-CA** exhibits absorbance maxima at 425 nm whereas **PY-PH** showed peaks at 450 nm, respectively. The value of the solid **PY-CA** film is 25 nm red shifted compared to the solution measurement. Thin film PL measurement of **PY-CA** and **PY-PH** showed PL maxima at 485 nm and 520 nm respectively. The optical band gap of these materials were measured by using spin coated thin films of **PY-CA** and **PY-PH** compounds from chloroform solution directly on ITO coated glass .The thin film optical data on ITO coated glass for **PY-CA** and **PY-PH** are shown in Figure 3. The optical band gap light absorption onset was determined by extrapolating the steepest slope to the intersection of the absorption baseline (substrate). The band gap for **PY-CA** and **PY-PH** are 2.67 eV and 2.50 eV, respectively. The observed optical band gaps are in a good agreement with our earlier reported thienothiophene substituted pyrene Py-TtC9 (2.44 eV) [24] and naphthalene substituted pyrene PY-1 (2.83 eV) [25] analogous compounds.

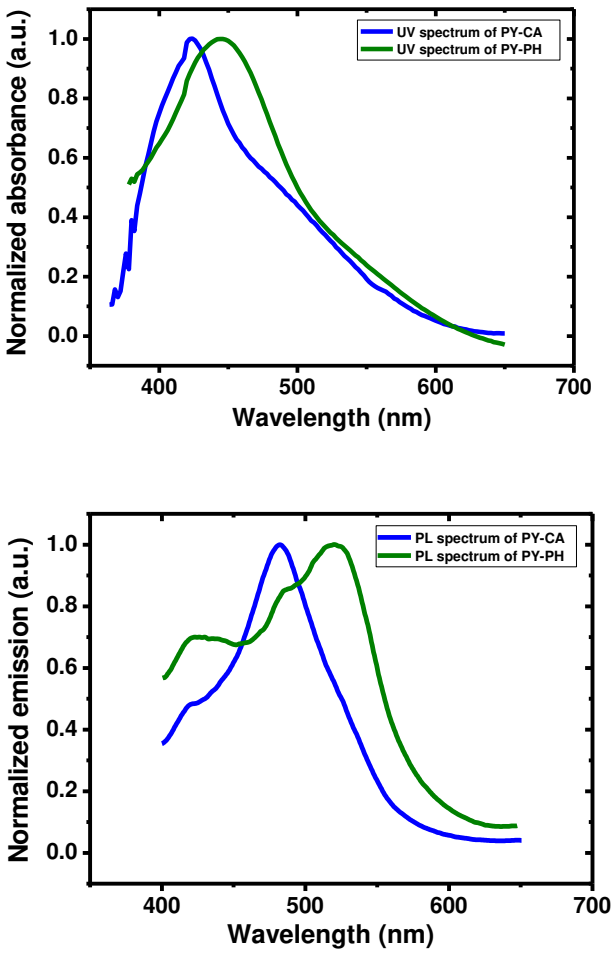

Figure 2. UV-vis absorption (upper) and photoluminiscence (lower) spectra of **PY-CA** and **PY-PH** compounds in thin film.

The higher band gap value of **PY-CA** and **PY-PH** is a clear sign of the wide band gap blue-green emitters. The energy levels of **PY-CA** and **PY-PH** organic semiconductors were characterized by the photoelectron spectroscopy in air (PESA) as shown in Figure 4. Thin films of **PY-CA** and **PY-PH** were deposited on the ITO coated glass by spin coating, which were used for the determination the ionization potential. The photoelectron yield ratio was measured with respect to the applied UV-energy. The onset point or slope across this graph gave the HOMO value of these materials.[30, 31] The HOMO value for the **PY-CA** and **PY-PH** are 5.48 eV and 5.40 eV, as recorded by PESA. The lower HOMO values of **PY-CA** and **PY-PH** are significant for making air stable organic electronic devices. The higher HOMO of **PY-PH** compared to **PY-CA** is again attributed to the extended conjugated moiety and electron rich sulfur of phenothiazine. This observation is in good agreement with optical red shift and optical band gap measured for **PY-PH**.

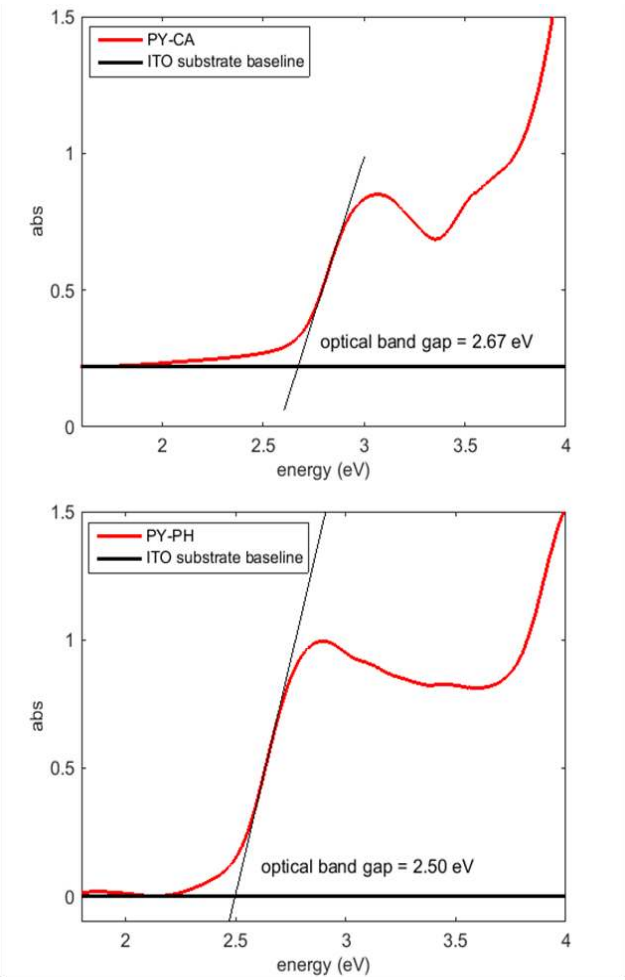

Figure 3. Optical band gap calculated using a thin film of **PY-CA** (upper) and **PY-PH** (lower) spin coated on the ITO coated glass substrates.

Density Functional Theory (DFT)[32] calculations were performed to compute molecular structures, the energies of frontier orbitals and their localization as well as absorption and photoluminescence (PL) spectra. The B3LYP [33] and CAM-B3LYP [34] exchange-correlations functionals were used with the 6-31g(d,p) basis set. These B3LYP and CAM- B3LYP correlations functionals were used because B3LYP provides more reliable HOMO (highest occupied molecular orbital) and LUMO (lowest unoccupied molecular orbital) energies which can be compared to the measured redox levels, while the range-separated CAM-B3LYP is preferred for optical properties involving transitions with significant degree of charge transfer.

(a)

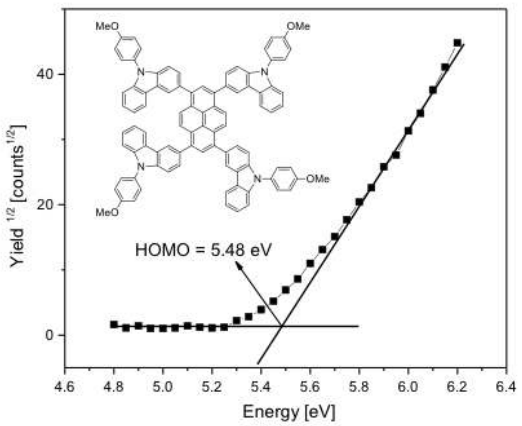

(b)

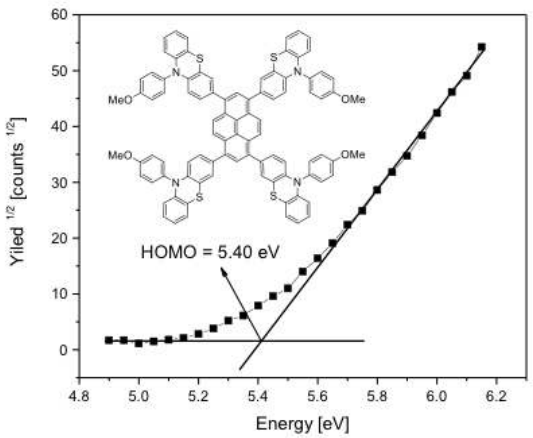

Figure 4 Photoelectro spectroscopy in air (PESA) analysis of compound **PY-CA** (a) and **PY-PH** (b) compounds in thin film.

The absorption and PL spectra were computed with time-dependent DFT (TD-DFT). [35] The PL spectra were computed by optimizing the first excited state. The calculations were performed in chloroform with the PCM (polarizable continuum model) [36] model of the solvent. All calculations were performed using Gaussian 09. [37] The HOMO and LUMO of **PY-PH** and **PY-CA** are shown in Figure 5 and Figure 6, respectively. In both comopunds, the HOMO is more delocalized than the LUMO and has appreciable amplitude on the phenothiazine and carbazole moieties, respectively, while the LUMO is more localized on the

central fused pyrene core and partially on the fused backbone of the PH or CA units. This also means that there is an appreciable degree of charge transfer in the transition responsible for the first peak in the absorption and PL spectrum (which we confirmed is mostly due to HOMO → LUMO) which calls for the use of a range-separated hybrid functional in the analysis of optical properties. [38, 39] The calculated HOMO and LUMO energies of **PY-CA** are -4.82 eV and -1.63 eV whereas for **PY-PH**, they are -4.79 eV and -1.79 eV, respectively. The higher HOMO value for **PY-PH** compared to **PY-CA** is related to the longer conjugation length of phenothiazine over carbazole. The HOMO-LUMO band gap for **PY-CA** and **PY-PH** was calculated to be 3.18 eV and 3.0 eV, respectively. The computed contraction of the band gap in **PY-PH** vs **PY-CA** of 0.18 eV matches well with the experimentally measured difference in optical band gaps of 0.17 eV.

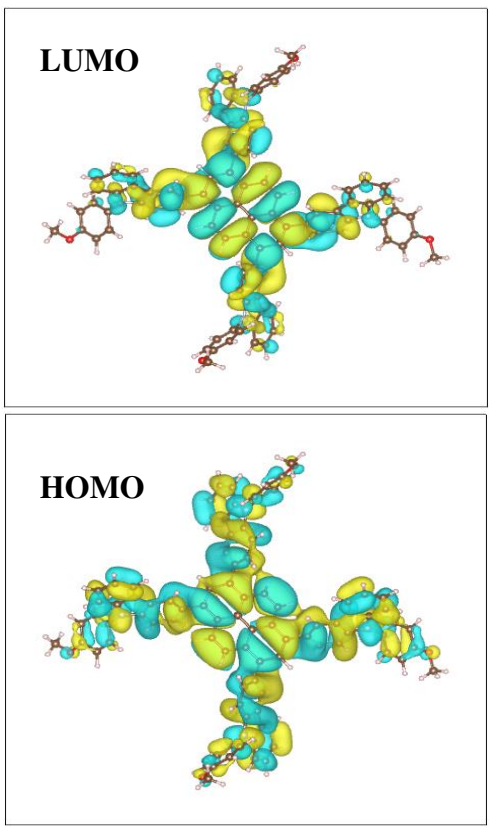

Figure 5. The electron density isocontours of HOMO and LUMO of **PY-CA** obtained at the CAM-B3LYP level (visualization of orbitals here and elsewhere by VESTA). [41]

The absorption peak maximum computed with CAM-B3LYP/B3LYP is 379/437 nm for **PY-CA** and 389/471 nm for **PY-PH**. The absorption spectra are shown in the Supporting Information. The peaks computed using the two functionals therefore straddle the measured peaks at 400 and 450 nm of **PY-CA** and **PY-PH**, respectively (vide infra). This is expected, as B3LYP is known to underestimate the excitation energy for large conjugated systems and CAM-B3LYP to often overestimate it. [40] These calculations confirm the red shift of the peak with phenothiazine vs carbazole which is observed experimentally. The red shift was also confirmed for PL: the computed PL peaks were 471 and 538 nm for **PY-CA** and **PY-PH**, respectively (CAM-B3LYP, see Supporting Information). In order to test the electroluminescent properties of **PY-CA** and **PY-PH** materials, we used them as an active emissive layer in OLED devices.

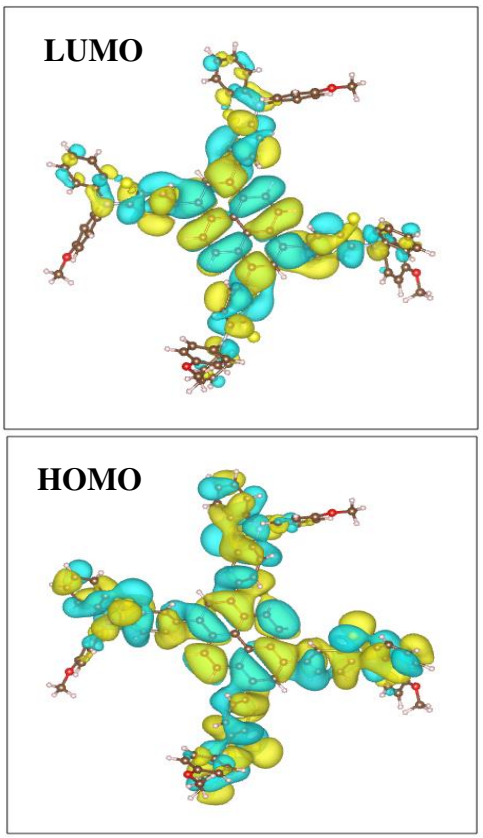

Figure 6. The electron density isocontours of HOMO and LUMO of **PY-PH** obtained at the CAM-B3LYP level.

The device configurations of compounds **PY-CA** and **PY-PH** are ITO/PEDOT:PSS(50nm)/**PY-CA** (50 nm)/TPBi (20 nm)/Ca (20 nm)/Ag (100) and ITO/PEDOT:PSS(50nm)/**PY-PH** (50 nm)/TPBi (20 nm)/Ca (20 nm)/Ag (100) respectively (see Figure 7). ITO coated glass and calcium with silver act as anode and cathode respectively whereas 2,2',2"-(1,3,5-benzinetriyl)-tris(1-phenyl-1-H-benzimidazole) (TPBI) is an electron transporting layer. When a potential is applied, holes are injected from anode and electrons injected from the cathode respectively. Due to the recombination of holes and electrons in the active emissive layer, blue and green photon emission was observed in OLED devices. The observed electroluminescence (EL) was recorded as shown in Figure 7, while the EL performance data are given in Table 1. The **PY-CA** device has an EL maximum of 493 nm emission peak in the visible blue region with a full wave half maximum (FWHM) of 80 nm and CIE coordinates of 0.19 and 0.42. While the **PY-PH** device has an EL maximum of 540 nm in the visible green region with a FWHM of 85 nm and CIE coordinates of 0.37 and 0.59. The **PY-CA** device shows turn on voltage (V_{on}),

maximum current efficiency (CE_{max}), maximum power efficiency (PE_{max}), maximum brightness (MB_{max}) of 3.3 V, 1.6 cd/A, 1.5 lm/W and 2500 cd/m^2, respectively. Whereas the **PY-PH** device exhibits V_{on}, CE_{max}, PE_{max} and MB_{max} of 3.8 V, 1.1 cd/A, 0.45 lm/W and 2116 cd/m^2. The power efficiency of the **PY-CA** device is almost three times higher (1.5 lm/W) than the **PY-PH** device (0.45 lm/W). The CE and PE characteristic of the **PY-CA** and the **PY-PH** device is shown in Figure 8.

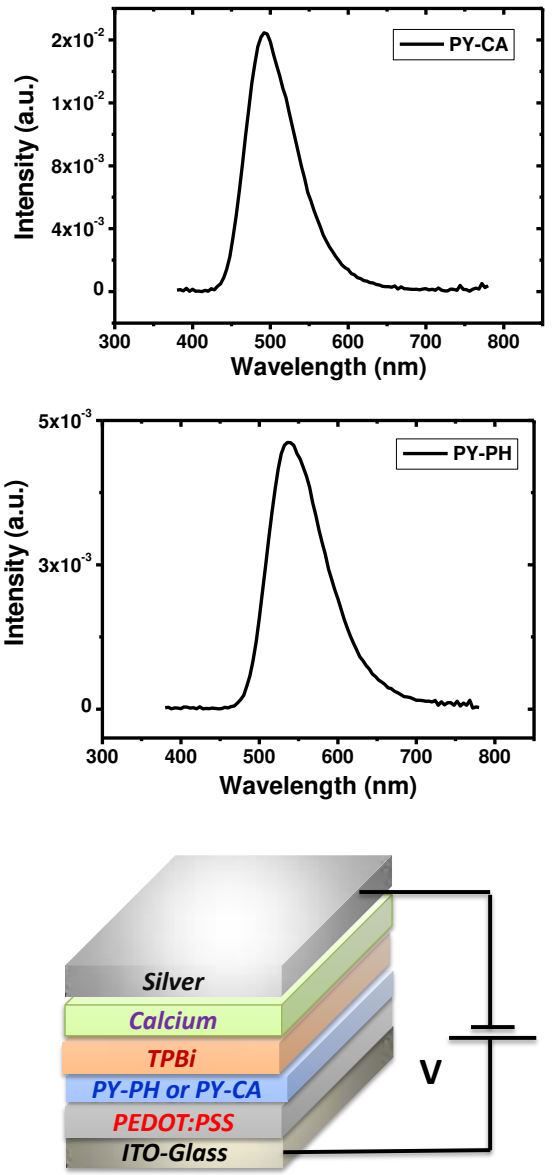

Figure 7. Carbazole substituted pyrene **PY-CA** (upper) and phenothiazine substituted pyrene **PY-PH** (middle) based electroluminiscent spectrum and **PY-CA** or **PY-PH** light emitting layer deposited OLED device structure (lower).

As the voltage increase from 3 V to 4 V, both the CE and PE of the **PY-CA** device increase rapidly to the CE_{max} and the PE_{max} of 1.6 cd/A and 1.5 lm/W respectively. As the drive voltage further increases, the CE and PE curves of the **PY-CA** device roll-off less rapidly. However, the CE and PE of the **PY-CA** device still remain at higher than one-half of the CE_{max} and PE_{max} even as the drive voltage is increased from 4 V to 11 V and 7.5 V, respectively. As the voltage increases from 3.8 V to around 8 V, both the CE and PE of the **PY-PH** device increase gradually to the CE_{max} and the PE_{max} of 1.1 cd/A and 0.45 lm/W, respectively. Unlike the case of the **PY-CA** device, the CE and PE curves of the **PY-PH** device roll-off more rapidly, the CE and PE drop to one-half of the CE_{max} and PE_{max} when the drive voltage is increased from 8 V to 10 V. The overall higher performance of **PY-CA** than **PY-PH** is attributed to the appropriate energy levels for hole injection, better charge transporting and carrier mobility. The observed OLED performances for both compounds are much better than our previously reported naphthalene substituted pyrene derivatives.[25] The stable blue color output additionally proves that **PY-CA** has high prospective to be a blue emitter in OLED applications. The turn on voltage of 3.3 V also makes **PY-CA** based OLED device energy efficient.

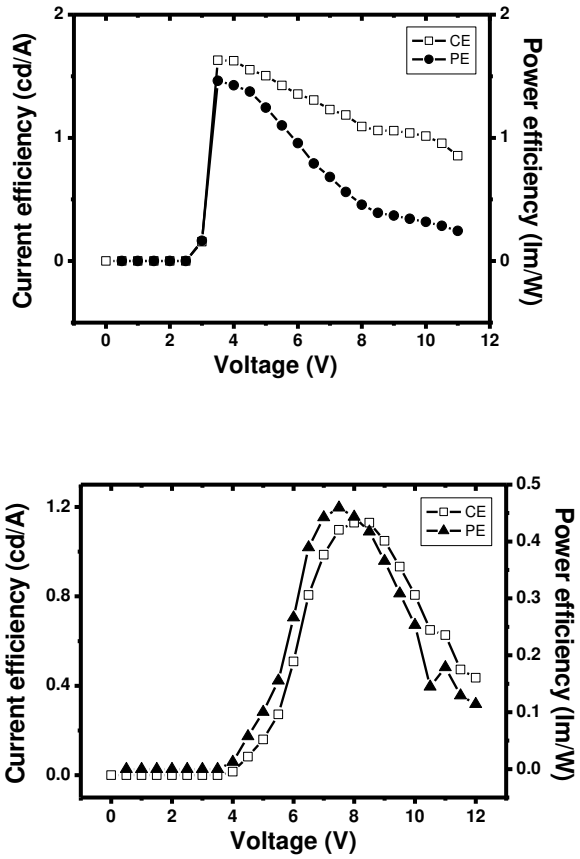

Figure 8. CE and PE characteristic of the **PY-CA** device (upper) and the **PY-PH** device (lower).

The morphological behavior of **PY-CA** and **PY-PH** active layer thin film was characterized by atomic force microscopy (AFM) as shown in Figure 9. The measured root mean square (RMS) roughness of film samples was 2.32 nm for **PY-CA** and 1.06 nm for **PY-PH**. The pristine ITO coated glass showed high surface roughness with an RMS of 3.25 nm. Smooth film morphology of

Cite this: DOI: 10.1039/c0xx00000x

www.rsc.org/xxxxxx

ARTICLE TYPE

Table1. Electroluminescent performance summary of **PY-PH** and **PY-CA** based OLED device

Device	Turn on Voltage (V)	Current Efficiency (Cd/A)	Power Efficiency (lm/W)	CIE	Electroluminescent Peak (nm)	Max. Brightness (cd/m2)
PY-CA	**3.3**	**1.6**	**1.5**	**(0.19,0.42)**	**493**	**2500**
PY-PH	**3.8**	**1.1**	**0.45**	**(0.37, 0.59)**	**540**	**2116**

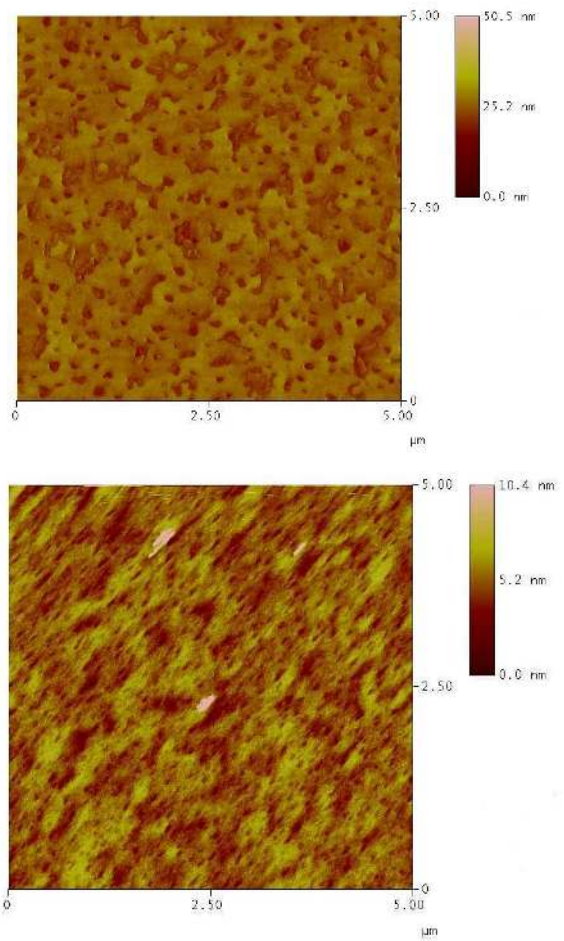

Figure 9. Atomic force microscope images of **PY-CA** (upper) and **PY-PH** (lower) spin coated thin film on ITO coated glass.

PY-PH film compared to **PY-CA** might be attributed to the more bulky phenothiazine group compared to carbazole moiety. This is also one of the reasons why **PY-CA** exhibited better OLED performance than **PY-PH** counterpart. The AFM images of **PY-CA** and **PY-PH** clearly demonstrated the amorphous nature of the thin film with complete coverage of microstructure domains on the thin film. Thin film morphology plays crucial role for light emission in terms of transportation of holes and electrons in recombination zone.

Conclusions

In summary, we have successfully designed and synthesized a new solution processable 1, 3, 6, 8- tetrasubstituted pyrene based electroluminescent organic semiconductors namely **PY-CA** and **PY-PH** via Suzuki coupling. **PY-CA** and **PY-PH** exhibited wide UV-vis absorption starting in the region 300 nm to 500 nm with an optical band gap of 2.67 eV and 2.50 eV, respectively. The HOMO values of **PY-CA** and **PY-PH** thin films were determined using PESA and were found to be 5.48 eV and 5.40 eV respectively. **PY-CA** and **PY-PH** were used for OLED device applications and their electroluminescence properties were studied. The turn on voltage for both the devices was calculated in the range of 3.3 V to 3.8 V. **PY-CA** exhibited blue emission with electroluminescent peak at 493 nm, maximum brightness around 2500 cd/m^2 and power efficiency of 1.5 lm/W whereas **PY-PH** shows green emission with electroluminescent peak at 540 nm, maximum brightness around 2116 cd/m^2 and power efficiency of 0.5 lm/W. The reported OLED data clearly indicate that this class of functional materials hold a great promise for designing future cost effective and efficient light emitting materials for OLED devices. Further enhancements are expected to obtain improved performance with optimized molecular and device structure for OLED displays.

Acknowledgements

F. L. Wong, V. A. L. Roy is thankful to the Research Grants Council of the Hong Kong Special Administrative Region (Project No. T23-713/11). PS thanks to Queensland University of

Technology (QUT) and Australian Research Council (ARC) for financial support (FT130101337). S.M. thanks to the Ministry of Education of Singapore (AcRF grant). KF thanks the Australian Renewable Energy Agency for financial support.

Notes and references

[a]*Polymer Science and Engineering Division, CSIR-National Chemical Laboratory, Dr. Homi Bhabha Road, Pune 411008, India.*

[b]*Current Address: Department of Chemistry and Bioengineering, Tampere University of Technology, P.O. Box 541, FI-33101 Tampere, Finland*

[c]*Center of Super Diamond and Advanced Films, and Department of Physics and Materials Science City, University of Hong Kong, Tat Chee Avenue, Kowloon, Hong Kong*

[d]*CSIRO Energy Centre10 Murray Dwyer Circuit Mayfield West NSW 2304, Australia*

[e]*Department of Mechanical Engineering Faculty of Engineering, National University of Singapore Block EA #07-08, 9 Engineering Drive 1, Singapore 117576*

[f]*School of Chemistry, Physics and Mechanical Engineering, Queensland University of Technology(QUT), Brisbane, Australia*

†Electronic Supplementary Information (ESI) available: NMR, MALDI-TOF MS data of compounds **2**, **3**, **4**, **5**, **6**, **7**, **8**, **PY-CA** and **PY-PH** See DOI: 10.1039/b000000x

References

1. C. W. Tang, S. A. Vanslyke, *Appl. Phys. Lett*. 1987 , **51** , 913
2. A. C. Grimsdale, K. L. Chan, R. E. Martin, P. G. Jokisz and A. B. Holmes, *Chem. Rev*., 2009, **109**, 897.
3 L. S. Hung, C.H. Chen, *Mat. Sci. Eng*., R 2002 , **39** , 143.
4. J. Kido and Y. Okamoto, *Chem. Rev*., 2002, **102**, 2357.
5. H.Uoyama, K. Goushi, K.Shizu, H. Nomura, C. Adachi, *Nature*, 2012, **492**, 234.
6. Y. H. Kim, H. C. Jeong, S. H. Kim, K. Yang, S. K. Kwon, *Adv. Funct. Mater*. 2005, **15**, 1799.
7. Z. J. Zhao, S. M. Chen, J. W. Y. Lam, P. Lu, Y. C. Zhong, K. S. Wong, H. S. Kwok, B. Z. Tang, *Chem. Commun*. 2010, **46**, 2221.
8. X. Kong, A. P. Kulkarni, S. A. Jenekhe. *Macromolecules* 2003, **36**, 8992.
9. K. R. J. Thomas, M Velusamy, J. T. Lin, Y. T. Tao, H. Chuen, *Adv. Funct. Mater*. 2004, **14**, 387-392.
10. *Organic Light-Emitting Devices: Synthesis, Properties, and Applications*, ed. K. Muellen and U. Scherf, Wiley-VCH, 2006, vol. 978.
11. Z. Ma, P. Sonar and Z. K. Chen, *Curr. Org. Chem*., 2011, **14**, 2034.
12. J. N. Moorthy, P. Natarajin, P. Venkatakrishnan, D. F. Huang and T. J. Chow, *Org. Lett*., 2007, **9**, 5215.
13. M. Y. Lo, C. G. Zhen, M. Lauters, G. E. Jabbour, A. Sellinger, *J. Am. Chem. Soc*., 2007, **129**, 5808.
14. R. D. Xia, W. Y. Lai, P. A Levermore, W. Huang, D. D. C. Bradley, *Adv. Funct. Mater*., 2009, **19**, 2844.
15. Z. J. Zhao, J. H. Li, X. P. Chen, X. M. Wang, P. Lu, Y. Yang, *J. Org. Chem*., 2009, **74**, 383.
16. H. J. Zhang, Y. Wang, K. Z. Shao, Y. Q. Liu, S. Y. Chen, W. F. Qiu, X. B. Sun, T. Qi, Y. Q. Ma, G. Yu, Z. M. Su, D. B. Zhu, *Chem. Commun*., 2006, 755.
17. M. J. Sienkowska, J. M. Farrar, F. Zhang, S. Kusuma, P. A. Heiney and P. Kaszynski, *J. Mater. Chem*., 2007, **17**, 1399.
18. F. Liu, W. Y. Lai, C. Tang, H. B. Wu, Q. Q. Chen, B. Peng, W. Wei, W. Huang and Y. Cao, *Macromol. Rapid Commun*., 2008, **29**, 659.
19. Y. Sagara, T. Mutai, I. Yoshikawa and K. Araki, *J. Am. Chem. Soc*., 2007, **129**, 1520.
20. N. J. Jeon, J. Lee, J. H. Noh, M. K. Nazeeruddin, M. Grätzel, S. Seok, *J. Am. Chem. Soc*. 2013, **135**, 19087
21. J. B. Birks, *Photophysics of Aromatic Molecules, Wiley-Interscience*, London, 1970.
22. J. R. Lackowicz, *Principles of Fluorescence Spectroscopy*, Kluwer Academic/Plenum Publishers, New York, 2 edn, 1999, pp. 595
23. M. T. Figueira-Duarte, K. Mullen. *Chem. Rev*. 2011, **111**, 7260.
24. P. Sonar, M. S. Soh, Y. H. Cheng, J. T. Henssler, A. Sellinger, *Org. Lett.*, 2010, **12**, 3292.
25. J. K. Salunke, P. Sonar, F. L. Wong, V. A. L. Roy, C. S. Lee, P. P. Wadgaonkar, *Phys. Chem. Chem. Phys*., 2014, **16**, 23320.
26. S. J. Lee, J. S. Park, K.-J. Yoon, Y.-I. Kim, S.-H Jin, S. K. Kang, Y.-S. Gal, S. K., J. Y. Lee, J.-W. Kang, S-H. Lee, H.-D. Park, J.-J. Kim *Adv. Funct. Mater.* 2008, **18**, 3922-3930.
27. G. B. Bodedla, K. R. J. Thomas, S. Kumar, J.-H. Jou. C.-J. Li. *RSC Adv.,* 2015, **5**, 87416-87428.
28. A. Matoliukstyte, J.V. Grazulevicius, J.A. Reina, V. Jankauskas , E. Montrimas, *Mater. Chem. Phys.,* 2006, **98**, 324.
29. J. H. Huang, K. C. Lee *ACS Appl. Mater. Interfaces* 2014, **6**, 7680−7685
30. J. Jasieniak, M. Califano, S. E. Watkins, *ACS Nano*, 2011, **5**, 588
31. M. Onoda, K. Tada, H. Nakayama, *J. Appl. Phys*. 1999, **86**, 1999.
32. W. Kohn, L. J. Sham, *Phys Rev*, 1965, **40**, A1133.
33. A.D. Becke, *J. Phys, Chem*., 1993, 5648
34. T. Yanai, D. Tew, N. Handy, *Chem. Phys. Lett*., 2004, **393**, 51.
35. M. A. L. Marques MAL, *Annu. Rev. Phys. Chem*., 2004, **55**, 427.
36. J. Tomasi, B. Mennucci, R. Cammi, *Chem. Rev*., 2006, **105**, 2999.
37. M. J. Frisch (2009) Gaussian 09. Gaussian Inc., Wallingford.
38. M. J. G. Peach, P. Benfield, T. Helgaker, D.J. Tozer, *J. Chem. Phys*. 2008, **128**, 044118.
39. S. Manzhos, H. Segawa, K. Yamashita, *Chem. Phys. Lett.* 2013, **527**, 51.
40. D. Jacquemin, V. Wathelet, E. A. Perpete, C. Adamo, *J. Chem. Theory Comput.*, 2009, **5**, 2420.
41. K. Momma, F. Izumi, *J. Appl. Crystallogr*., 2011, **44**, 1272.

